Konf. Aspirantov (*Rostov-on-Don*: *Rostov Sk. Univ.*) Sb, p. 61. (English abstract).

MYASNIKOVA, T. P. & AREFEV, I. M. (1964). *Optika i Spektroskopiya*, **16**(3), 540. (English translation).

MYASNIKOVA, T. P. & YATSENKO, A. F. (1962). *Sov. Phys. Solid State*, **4**, 475.

NELMES, R. J. (1969). Ph. D. Thesis. Edinburgh University.

NELMES, R. J. (1970). *J. Appl. Cryst.* **3**, 422.

ODEN, L. L. (1966). *Dissertation Abstracts*, **26**(7), 3654.

PEPINSKY, R., VEDAM, K., HOSHINO, S. & OKAYA, Y. (1958). *Phys. Rev.* **111**, 1508.

PEPINSKY, R. & VEDAM, K. (1960). *Phys. Rev.* **117**, 1502.

POST, B. (1969). *Acta Cryst.* A **25**, 94.

QURASHI, M. M. (1963). *Acta Cryst.* **16**, 307.

RUSH, J. J. & TAYLOR, T. I. (1965). *Inelastic Scattering of Neutrons*, Vol. II, p. 333. Vienna: International Atomic Energy Agency.

SMITH, J. A. S. (1968). Private communication.

SRIVASTAVA, R. C. & LINGAFELTER, E. C. (1966). *Acta Cryst.* **20**, 918.

STEWART, R. F., DAVIDSON, E. R. & SIMPSON, W. T. (1965). *J. Chem. Phys.* **42**, 3175.

STRUKOV, B. A. & DANILYCHEVA, M. N. (1963). *Sov. Phys. Solid State*, **5**, 1253.

STRUKOV, B. A., KOPTSIK, V. A. & LIGASOVA, V. D. (1962). *Sov. Phys. Solid State*, **4**, 977.

TEMPLETON, D. H. (1962). In *International Tables for X-ray Crystallography*. Vol. III, p. 213. Birmingham: Kynoch Press.

Anisotropy of the Sodium Atom in Low Albite

BY S. QUARENI

Istituto di Mineralogia e Petrografia, Universita di Padova, Italy

AND W. H. TAYLOR

Crystallographic Laboratory, Cavendish Laboratory, Cambridge, England

Measurements of diffraction intensities at elevated temperatures have been used to study the anisotropy of the sodium atom in low albite. The new observations provide strong support for the interpretation of the observed anisotropy in terms of anisotropic thermal vibration of the atom.

1. Introduction

In both low albite and high albite the electron density distribution around the sodium atom is markedly anisotropic, the atom appearing to be elongated (Ferguson, Traill & Taylor, 1958; Ribbe, Ferguson & Taylor, 1962; Ribbe, Ferguson, Traill & Taylor, 1963). In high albite the anisotropy is very large and probably corresponds to the space-average of a multipartite structure with faulted domains. In low albite the much smaller anisotropy is probably to be interpreted as the time-average of the anisotropic thermal vibration of the sodium atom, though the evidence is not sufficiently conclusive to rule out the possibility of a space average of the kind proposed for high albite (Ribbe, Megaw & Taylor, 1969).

The most direct way of deciding whether the anisotropy of the sodium atom in low albite represents true anisotropic thermal vibration or a space average is to study the anisotropy over a wide range of temperature. For on any physically reasonable model of the variation of thermal vibration with temperature the amplitude of vibration must be reduced at lower temperatures, increased at higher temperatures. An earlier inconclusive study at $-180°$C (Williams, 1961; Williams & Megaw,

1964) was taken into account by Ribbe, Megaw & Taylor (1969) in their discussion of the anisotropy in low albite. The experiments now reported have given information about the anisotropy at 300 and 600°C, and when combined with a re-examination of the measurements of Williams (1961) leave little doubt that in low albite the observed anisotropy of the sodium atom represents true anisotropic thermal vibration.

2. Experimental measurements

A sample of low albite from the Schmirntal, Tyrol, was obtained from the Gasser collection in the Mineralogical Museum of the University of Padua.

Axial lengths and interaxial angles of the conventional base-centred unit cell (space group $C\bar{1}$) were determined at 20, 300 and 600°C, using a precession camera calibrated with quartz and sodium chloride. They are listed in Table 1, together with the average expansion coefficient over the range 20–600°C for each of the axes a, b, c.

The major axis of the elongated sodium atom lies very nearly in the plane (100), so that a two-dimensional projection on this plane offers the simplest method of studying the variation of anisotropy with temperature.

Diffraction intensities for reflexions $\{0kl\}$ from a fragment $0.12 \times 0.12 \times 0.18$ mm, elongated along **a**, were recorded photographically for the sequence of temperatures, 20, 300, 600, 20° C. The normal multiple-film technique was used with filtered Mo $K\alpha$ radiation to obtain $\{0kl\}$ reflexions on zero-layer photographs in a high-temperature integrating Weissenberg goniometer (Quareni, 1969). To avoid the risk of contaminating the albite crystal through the use of a refractory cement in mounting, the crystal was sintered on the platinum–platinum/rhodium thermocouple by heating for 20 minutes at 1000° C (Quareni, 1969); after this short period of heating the albite remains in the low-temperature form.

In this way 153 measurable independent $\{0kl\}$ reflexions were recorded at 20° C, 133 at 300° and 117 at 600°. The strong and medium intensities were measured on a flying-spot microdensitometer (Joyce–Loebl), the weak reflexions by visual comparison with a standard scale prepared in the usual way from the same crystal fragment. Intensities were corrected for Lorentz and polarization effects, but no absorption correction was required for this small crystal used with Mo $K\alpha$ radiation.

Structural computations were performed on the TITAN computer in the University Mathematical Laboratory, Cambridge, using programs written by Mrs J. C. Matthewman. Atomic scattering factors were computed for fully ionized atoms from the analytical expression of Forsyth & Wells (1959), using their coefficients for Na^+, Al^{3+} and Si^{4+} and coefficients given by Tokonami (1965) for O^{2-}. Perfect Al,Si order was assumed, therefore all the Al^{3+} was allocated to site $T_1(0)$, the remaining T sites being occupied by Si^{4+}.

3. Refinement of the structures

The atomic coordinates for low albite obtained in the very accurate three-dimensional analysis of Ribbe, Megaw & Taylor (1969) were used as the starting point for the refinement of the structure derived from each set of experimental measurements, one at each of the four temperatures (20, 300, 600, 20° C) in the experiments described above. In the account which follows, attention is directed explicitly to the treatment of the sodium

atom, the refinement in regard to the other atoms following the usual routine.

The first stages of refinement were carried out by means of difference syntheses using a single Na^+ atom with isotropic temperature factor. To carry the refinement as far as possible, later stages were based on *either* the split-atom model *or* the anisotropic temperature factor model.

In the first, the single Na^+ atom was replaced by two $\frac{1}{2}Na^+$ atoms, each with its own isotropic temperature factor, separated by a suitable distance; least-squares refinement was then carried out until no further improvement in the R factor was obtained. The vector separation of the two half-atoms is then used as a measure of the anisotropy of the Na^+ atom [as in Williams & Megaw (1964) and in Ribbe, Megaw & Taylor (1969)], though it must be emphasized that this procedure carries no implication that the physical interpretation must be in terms of a space average.

The second model retains the single Na^+ atom, but replaces the isotropic temperature factor by an anisotropic temperature factor. Again the least-squares refinement procedure was followed in order to obtain the best possible R factor.

The results of the refinements are shown in Table 2, from which it is seen that the two models are about equally good if judged by the final R factor, as is also the case if difference syntheses are compared (Fig. 1). For any one of these structures, therefore, it would not be possible to assert that the anisotropic thermal vibration model is clearly distinguishable from the split-atom model, a result in line with Megaw's discussion in the Appendix to Ribbe, Megaw & Taylor (1969).

The important result which follows from the figures in Table 2 is that anisotropy of the sodium atom, as seen in the [100] projection, increases at higher temperatures, whether measured by the separation of the half-atoms in the split-atom model *or* by the root-mean-square component of the maximum displacement in the thermal vibration model. The conclusion to be drawn is that the anisotropy represents the time-average of a true anisotropic thermal vibration of the sodium atom within the cavity formed by adjacent oxygen atoms, rather than a space-average due to the location of

Table 1. *Low albite, Schmirntal. Cell dimensions, expansion coefficients*

Temperature (°C)	20	300	600	Error	Expansion coefficient
a (Å)	8·142	8·187	8·221	±0·006	17×10^{-6}
b (Å)	12·780	12·797	12·841	±0·009	8×10^{-6}
c (Å)	7·158	7·160	7·166	±0·005	2×10^{-6}
α	94° 10′	93° 50′	93° 32′	± 5′	
β	116° 35′	116° 32′	116° 25′	± 5′	
γ	87° 50′	87° 48′	87° 42′	± 5′	

Notes. Estimated limits of error are quoted, *not* standard deviations. Expansion coefficients are average values over the range 20–600 °C.
All measurements on the same material (Schmirntal).

sodium atoms at different points within that cavity in different unit cells.

4. Discussion of the structures

Extreme care is necessary if reliable conclusions are to be drawn from two-dimensional studies of structures as complicated as the felspars. In this connexion the following points should be considered in their bearing on the interpretation of the figures in Table 2.

(i) The experimental crystal, mounted by sintering (§ 2, above), remains in the low albite form. Direct confirmation that (to the accuracy of this study) *no* changes in the structure are produced by sintering was obtained by structure refinements carried out with measurements of $\{0kl\}$ intensities at 20°C before sintering and after sintering, using the split-atom model. The results are included in Table 2.

(ii) For the low albite (Schmirntal) used in these experiments four independent structure refinements at 20°C are available (first and last in the temperature sequence 20, 300, 600, 20°C for one fragment, before and after sintering for the second fragment) and all lead to a separation 0·40 Å between half-atoms in the split-atom model. This is significantly different from the separation 0·364 Å derived by Ribbe, Megaw & Taylor

(1969, p. 1506) in their three-dimensional study of low albite from Ramona, also at 20°C (room temperature).

The difference might reflect a real difference between the two materials, both low albites. To test this, the $\{0kl\}$ intensities extracted from the three-dimensional set for Ramona albite were refined by the same methods as in the present study with the result that the half-atom separation increased to 0·40 Å as for the Schmirntal material (Table 2). It is not possible to see exactly how the (more accurately-determined) 0·364 Å changes to the 0·40 Å of the two-dimensional analysis, though it seems clear that the difference must arise from overlap in projection on (100) of electron density from other atoms or from unsuspected diffraction effects due to the use of incomplete sets of diffraction intensities.

If, however, the anisotropic thermal vibration models are compared similarly (Table 2), there is now a possibly-significant difference between the r.m.s. components of the maximum thermal displacements for Schmirntal (0·30 Å) and Ramona when computed by the same methods from the two-dimensional data (0·27 Å); moreover the latter value is identical (to the accuracy of the present study) with the r.m.s. value, 0·26 Å, from the three-dimensional study (Ribbe, Megaw & Taylor, 1969, footnote to their Table 4). It is

Table 2. *Low albite. Representation of the sodium atom*

Split-atom model

	(S_1) y 20°C before sintering	z	(S_1) y 20°C after sintering	z
Na$_1$	0·977	0·170	0·977	0·171
Na$_2$	0·999	0·128	0·001	0·130
Average s.d. (Å)	0·025		0·024	
Separation (Å)	0·40 (3)		0·40 (3)	
R (%)	7·6		6·9	

Split-atom model

	(S_2) y 20°C	z	(S_2) y 300°C	z	(S_2) y 600°C	z	(RMT, 1969) y 20°C	z	(WM, 1964) y −180°C	z
Na$_1$	0·977	0·168	0·975	0·167	0·970	0·164	0·977	0·163	0·985	0·161
Na$_2$	0·999	0·126	0·002	0·124	0·003	0·125	0·001	0·125	0·994	0·132
Average s.d. (Å)	0·015		0·025		0·028		0·035		0·022	
Separation (Å)	0·40 (2)		0·46 (3)		0·50 (4)		0·40 (5)		0·22 (3)	
R (%)	6·8		6·2		6·2		7·5		9·9	

Anisotropic thermal vibration model

	(S_2) y 20°C	z	(S_2) y 300°C	z	(S_2) y 600°C	z	(RMT, 1969) y 20°C	z	(WM, 1964) y −180°C	z
Na	0·9869	0·1484	0·9873	0·1495	0·9866	0·1440	0·9905	0·1430	0·9801	0·1455
Average s.d. (Å)	0·003		0·005		0·006		0·016		0·010	
Displacement (Å)	0·30 (2)		0·37 (2)		0·40 (3)		0·27 (3)		0·15 (2)	
R (%)	6·4		6·2		6·2		7·9		9·6	

Notes. (1) Atomic parameters y and z for the sodium atom Na, or half-atoms Na$_1$ and Na$_2$, for Schmirntal first (S_1) and second (S_2) fragments, and for experimental measurements from Ribbe, Megaw & Taylor (1969) and Williams & Megaw (1964).

(2) Average standard deviations of atomic coordinates (in Å), separation between half atoms Na$_1$, Na$_2$ (in Å) and r.m.s. component of the maximum thermal displacement of the Na atom on the [100] projection (in Å).

(3) For Separation (in split atom model) or Displacement (in anisotropic thermal vibration model), figures in brackets are standard deviations and refer to the last decimal place.

possible, though not certain, that this difference in behaviour, when the same two-dimensional sets of intensities are subjected to the same computational procedures, directly reflects the physical superiority of the anisotropic thermal vibration model of the sodium atom in low albites.

(iii) Comparison of the results obtained in the present high-temperature study with those obtained by Williams (1961) and Williams & Megaw (1964) in their low-temperature examination of (Ramona) low albite is very instructive. Their refinement of the [100] projection at $-180°C$, using a split-atom model, was terminated at $R=11\cdot1\%$ when the separation of the $\frac{1}{2}Na$ atoms was $0\cdot27$ Å, already much smaller than the split-atom separation at $20°C$ ($0\cdot36-0\cdot40$ Å). The application to their measurements of the least-squares refinement procedure used in the high-temperature study reduced the R factor to $9\cdot9\%$, with reduction in the split-atom separation to $0\cdot22$ Å (Table 2). The same refinement procedures, applied to the same measurements, but using the anisotropic thermal vibration model, gave a slightly better R factor, $9\cdot6\%$, and r.m.s. maximum thermal displacement $0\cdot15$ Å.

The low-temperature measurements thus provide strong support for the conclusion drawn (§ 3) from the high-temperature measurements – that the anisotropy of the sodium atom in low albite represents a true anisotropic thermal vibration of the atom within its cavity in the structure.

5. Variation of isotropic temperature factor

If it is assumed that the variation with temperature of the isotropic temperature factor B for each kind of atom in albite is linear, as in simple structures under certain conditions, values of B measured at different temperatures should extrapolate to $B=0$ at $T=0°K$. If at $T=0$ it is found that $B>0$, it may be assumed that the 'effec-
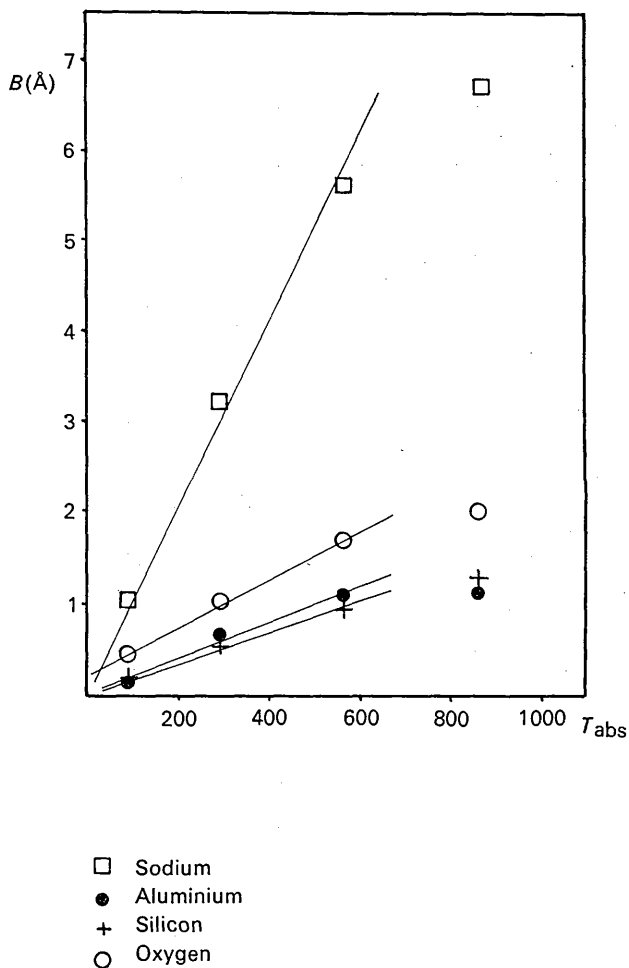

□ Sodium
● Aluminium
+ Silicon
○ Oxygen

Fig. 2. Isotropic temperature factor B (Å^2) *versus* temperature (°K) for sodium, aluminium, silicon and oxygen atoms.

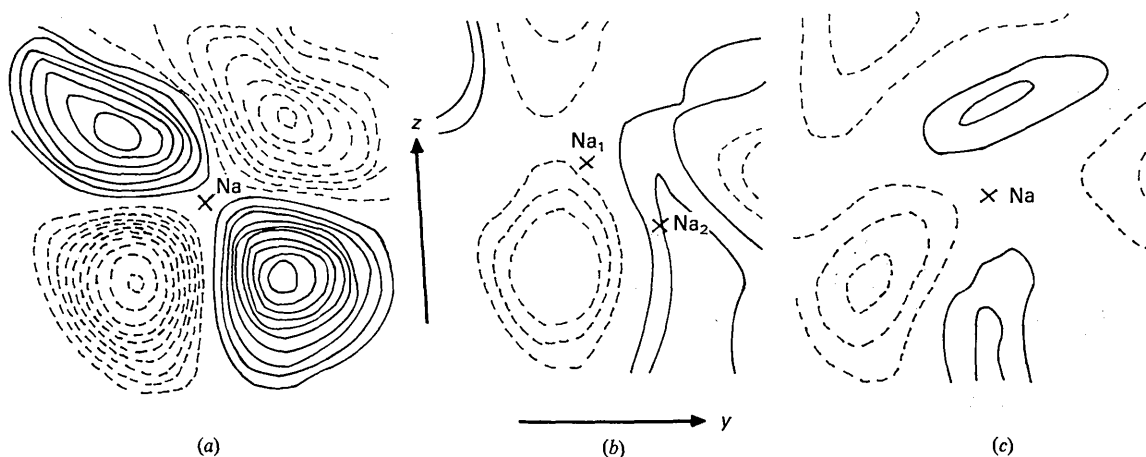(a)   (b)   (c)

Fig. 1. The anisotropy of the sodium atom at 20°C, shown in difference maps ($\varrho_0 - \varrho_c$) in [100] projection. (a) Single sodium atom, B_{Na} (isotropic) $= 3\cdot24$ Å^2. (b) Split-atom model, $B_{Na_1} = 1\cdot73$, $B_{Na_2} = 2\cdot12$ Å^2 (both isotropic). (c) Anisotropic thermal vibration model $\beta_{22} = 62$, $\beta_{33} = 217$, $\beta_{23} = -65$ (all × 10^{-4}).

tive temperature factor' represents not only true thermal vibration but also some spread in position of the atom due to spatial disorder.

Table 3 lists isotropic B values determined in the course of the refinement procedure for the measurements on Schmirntal albite at 20, 300 and 600°C, and on Ramona albite at $-180°C$ (Williams, 1961). When plotted against absolute temperature (Fig. 2) it is seen that for each kind of atom the $B–T$ variation is very closely linear in the range -180 to 300°C, so that extrapolation to $T=0$ is justified. For sodium, aluminium and silicon atoms the extrapolation gives values of B very close to 0, whereas for oxygen atoms (at $T=0$) $B>0$.

Table 3. *Low albite. Isotropic temperature factors B* (Å²)

	(WM, 1964) $-180°C$	(S_2) 20°C	(S_2) 300°C	(S_2) 600°C
Na	1·0 (3)	3·2 (1)	5·6 (1)	6·7 (2)
Al	0·15 (6)	0·72 (6)	1·04 (9)	1·1 (1)
Si (average)	0·18 (6)	0·63 (4)	0·94 (6)	1·20 (8)
O (average)	0·38 (6)	1·01 (6)	1·65 (7)	2·0 (1)

Notes. Standard deviations are in brackets and refer to the last figure given.
Measurements on Schmirntal second fragment (S_2) and from Williams & Megaw (1964).

The difference between Na, Al and Si on the one hand, and O on the other, may be taken as evidence in support of a model in which the *position* of the Na atom is as clearly defined as are the positions of Al and Si atoms at the centres of their tetrahedral groups. Its large anisotropy is then due to anisotropic thermal vibration, not to positional disorder. By contrast, the O atoms show some positional disorder arising from the differences in Si–O and Al–O bond lengths and incomplete Al,Si order.

6. Conclusion

Measurements of diffraction intensities from low albite at 300 and 600°C have been used to study the anisotropy of the sodium atom as seen in [100] projection. Comparison with previous studies at room temperature and at $-180°C$ provides strong support for the view that the observed anisotropy represents a true anisotropic thermal vibration of the sodium atom.

References

FERGUSON, R. B., TRAILL, R. J. & TAYLOR, W. H. (1958). *Acta Cryst.* **11**, 331.
FORSYTH, J. B. & WELLS, M. (1959). *Acta Cryst.* **12**, 412.
QUARENI, S. (1969). *Z. Kristallogr.* **128**, 294.
RIBBE, P. H., FERGUSON, R. B. & TAYLOR, W. H. (1962). *Norsk Geol. Tidsskr.* **42** (2), 152.
RIBBE, P. H., FERGUSON, R. B., TRAILL, R. J. & TAYLOR, W. H. (1963). *Proc. Geol. Soc. Amer. Ann. Meetings, New York,* 136A.
RIBBE, P. H., MEGAW, H. D. & TAYLOR, W. H. (1969). *Acta Cryst.* **B25**, 1503.
TOKONAMI, M. (1965). *Acta Cryst.* **19**, 486.
WILLIAMS, P. P. (1961). Ph. D. Thesis, Cambridge.
WILLIAMS, P. P. & MEGAW, H. D. (1964). *Acta Cryst.* **17**, 882.

The Molecular and Crystal Structure of Hippuric Acid

By HANS RINGERTZ

*Department of Medical Physics, Karolinska Institutet and Department of Radiology, Karolinska Sjukhuset, S-10401 Stockholm, Sweden*

Hippuric acid, $C_6H_5.CO.NH.CH_2.COOH$, crystallizes with four molecules in an orthorhombic unit cell with $a=8·874$, $b=10·577$, $c=9·117$ Å, space group $P2_12_12_1$. The structure has been determined by direct methods and refined by full-matrix least-squares computations. The final R value is 5·8%. The benzene ring, the peptide part and the carboxylic group are planar and twisted with respect to each other. The molecules are held together in three dimensions by one $O–H\cdots O$ and one $N–H\cdots O$ hydrogen bond to the peptide oxygen atom.

Introduction

Hippuric acid
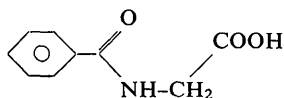
is formed in mammals when benzoic acid is detoxicated by conjugation with glycine. It is excreted in urine and constitutes about a half per cent of the nitrogen excretion in man. The crystallographic and optical data of hippuric acid have been given by Ringertz (1969).